

## PKS 2149–306 AND CXOCDFS J033225.3–274219: TWO AGNs WITH UNUSUAL SPECTRA POSSIBLY BLUESHIFTED?

D. BASU

Department of Physics, Carleton University, Ottawa, ON K1S 5B6, Canada; basu@physics.carleton.ca

Received 2004 July 29; accepted 2005 October 23

### ABSTRACT

PKS 2149–306 and CXOCDFS J033225.3–274219 each exhibit several emission lines in their optical spectra from which their redshifts have been determined. However, an *ASCA* spectrum of the first object has detected an emission line at 5 keV observed wavelength, and the *Chandra* ACIS-I spectrum of the second object shows a very strong emission feature at the observed wavelength of 6.2 keV. The two lines cannot be identified with any known search line on the basis of their redshift values without invoking extremely large outflow bulk velocities of  $0.6c$ – $0.75c$ . Such high bulk velocities are practically unheard of in any other observations of extragalactic objects. We show here that all the lines in both the optical and X-ray spectra of the two objects can be identified with lines at longer wavelengths that are blueshifted. We propose a scenario in which the spectrum is blueshifted due to net apparent motion toward the observer, resulting from an ejection.

**Key words:** cosmology: miscellaneous — galaxies: active — quasars: emission lines —  
 quasars: individual (PKS 2149–306, CXOCDFS J033225.3–274219) — X-rays: galaxies

### 1. INTRODUCTION

Two active galactic nuclei (AGNs) have been reported in recent years that exhibit very unusual spectra, in the sense that their redshifts have been determined on the basis of their optical emission lines, but an X-ray emission line subsequently discovered in each object cannot be identified.

PKS 2149–306 is a radio-loud (Jauncey et al. 1982) quasi-stellar object (QSO) with a reported redshift of 2.345 computed from its optical spectrum (Wilkes 1986). However, an emission line has been detected (Yaqoob et al. 1999) in the *ASCA* observation of this object at the emitted wavelength of 16.7 keV and with an emitted equivalent width of 0.3 keV (observed wavelength of 5.0 keV and observed equivalent width of 0.09 keV, based on the above redshift).

CXOCDFS J033225.3–274219 (J0332–274 for brevity) is an X-ray source detected in the Chandra Deep Field–South (Giacconi et al. 2002; Rosati et al. 2002) and is a radio-loud type 1 AGN. The optical counterpart lies at the contour center of the X-ray flux, and the optical spectrum led to the determination of its redshift, which was reported as 1.617 (Wang et al. 2003). However, the *Chandra* ACIS-I spectrum of the object exhibited a very strong emission feature at the observed wavelength of 6.2 keV and with an observed equivalent width of 4.4 keV (emitted wavelength of 16.2 keV and emitted equivalent width of 11.5 keV, based on the above redshift; Wang et al. 2003).

In neither of these two objects can the X-ray line be identified with any known line in the search list to match the respective redshift values, while the respective authors have completely ruled out any possibility that the line is an artifact or any instrumental effect. The occurrence of the line in each object has been attributed to the blueshifted Fe K emission line with a relativistic outflow velocity of  $\approx 0.6c$ – $0.75c$  (Yaqoob et al. 1999; Wang et al. 2003).

It is evident that the spectra of the two objects are extremely unusual and cannot be explained by the conventional redshift interpretation of observed spectra of extragalactic objects. On the other hand, the bulk velocities invoked by the respective authors to interpret the X-ray lines are practically unheard of in any other extragalactic object.

We therefore feel that it is worth exploring an alternative interpretation of the two spectra in terms of blueshifts. Blueshifts have successfully explained the spectra of extragalactic objects, viz., QSOs (Basu & Haque-Copilah 2001; Basu 2004), galaxies (Basu 1998, 2001a), host galaxies of gamma-ray bursts (Basu 2001b), and host galaxies of Type Ia supernovae (Basu 2000). The purpose of the present paper is to show that the emission features in the two AGNs PKS 2149–306 and J0332–274 can be explained in terms of blueshifts in the emission lines of the *entire* spectra, including both optical and X-ray features, and not as an inflow or outflow bulk velocity but as the motion of the object itself, which has been ejected and is thus *approaching* the observer.

The observed optical and X-ray spectra of PKS 2149–306 and J0332–274 are analyzed in § 2 in terms of blueshifts. Results are discussed in § 3. In § 4 we propose a scenario in which the spectrum is blueshifted due to the net motion toward the observer resulting from an ejection. Finally, some concluding remarks are presented in § 5.

### 2. BLUESHIFTED SPECTRA OF PKS 2149–306 AND J0332–274

The optical spectrum of PKS 2149–306 shows five broad emission lines, with peak wavelengths at 4073, 4131, 4694, 5162, and 6380 Å, identified in the redshift hypothesis as Ly $\alpha$   $\lambda$ 1216, Ne v  $\lambda$ 1240, O vi] + Si iv  $\lambda$ 1400, C iv  $\lambda$ 1549, and C iii]  $\lambda$ 1909, respectively (Wilkes 1986). An additional identification, Si ii  $\lambda$ 1264, is listed by Wilkes (1986), but no corresponding peak wavelength is given. It is therefore not considered a reliable observed line and is not included in the present analysis. The X-ray spectrum shows one emission feature at the observed wavelength of 5.0 keV, as mentioned earlier.

J0332–274 exhibits three broad emission lines in the optical spectrum at observed wavelengths of 4100, 5000, and 7312 Å (Wang et al. 2003). These have been identified in the redshift hypothesis as C iv  $\lambda$ 1549, C iii]  $\lambda$ 1909, and Mg ii  $\lambda$ 2798, respectively. The X-ray spectrum, as mentioned above, exhibits one line at the observed wavelength of 6.2 keV.

We have identified all the above lines in the blueshift scenario, with alternative search lines at longer wavelengths, and have

TABLE 1  
REDSHIFTS AND BLUESHIFTS IN THE SPECTRA OF PKS 2149–306 AND J0332–274

Object	$\lambda_o$	$W_o$	$z_r$ Line	$z_r$	$W_{er}$	$z_b$ Line	$z_b$	$W_{eb}$
2149–306 .....	4073	69	Ly $\alpha$ $\lambda$ 1216	2.3495	20.6	H $\alpha$ $\lambda$ 6563	0.3794	111.2
	4131?	35	N v $\lambda$ 1240	2.3315	10.5	He I $\lambda$ 6678	0.3814	56.6
	4694	8	O vi]+Si iv $\lambda$ 1400	2.3529	2.4	O I $\lambda$ 7772	0.3960	13.2
	5162	30	C iv $\lambda$ 1549	2.3325	9.0	O I $\lambda$ 8449	0.3890	49.3
	6380	...	C iii] $\lambda$ 1909	2.3421	...	He II $\lambda$ 10124	0.3698	...
	$5^{+0.2}_{-0.1}$	0.09	? $\lambda$ 16.73 $^{+0.52}_{-0.48}$	2.345?	0.3	Ar K $\alpha$ $\lambda$ 2.9567	0.4087	0.05
0332–274 .....	4057	...	C iv $\lambda$ 1549	1.6191	...	He I $\lambda$ 10830	0.6254	...
	5000	...	C iii] $\lambda$ 1909	1.6192	...	P $\beta$ $\lambda$ 12818	0.6099	...
	7358	...	Mg II $\lambda$ 2798	1.6297	...	P $\alpha$ $\lambda$ 18751	0.6076	...
	$6.2^{+0.2}_{-0.1}$	4.4	? $\lambda$ 16.2 $^{+0.5}_{-0.3}$	1.617?	11.5	S K $\alpha$ $\lambda$ 2.3066	0.6280	1.6

NOTES.—Wavelengths of optical lines are in angstroms, and those of X-ray lines are in keV;  $\lambda_o$  and  $W_o$  are the observed wavelength and observed equivalent width;  $W_{er}$  and  $W_{eb}$  are emitted equivalent widths calculated on the basis of redshifts and blueshifts; and  $z_r$  and  $z_b$  are search lines identified under the redshift and blueshift hypotheses, respectively. Data are from Wilkes (1986; optical) and Yaqoob et al. (1999; X-ray) for PKS 2149–306 and from Wang et al. (2003; optical and X-ray) for J0332–274.

computed blueshift values for every line. The standard procedure has been followed in the identification process (Basu 1973a, 1973b), in the sense that a “shift” (red or blue) is confirmed only if a minimum of two observed lines, whether in emission or absorption spectra, show the same value when identified with two separate search lines; and any additional observed lines must also obey this value.

In the blueshift scenario, the optical lines of PKS 2149–306 are identified as H $\alpha$   $\lambda$ 6563, He I  $\lambda$ 6678, O I  $\lambda$ 7772, O I  $\lambda$ 8449, and He II  $\lambda$ 10124. The X-ray feature, which failed to be identified in the redshift hypothesis, is interpreted in the blueshift hypothesis as Ar K $\alpha$   $\lambda$ 2.9567. The optical lines of J0332–274 are identified with He I  $\lambda$ 10830, P $\beta$   $\lambda$ 12828, and P $\alpha$   $\lambda$ 18751, respectively. The X-ray line, which cannot be identified in the redshift scenario, has been identified in the blueshift scenario as S K $\alpha$   $\lambda$ 2.3066. In addition, we have computed rest-frame equivalent widths of the lines, in both the redshift and the blueshift hypotheses, for which observed equivalent widths are available. Results are shown in Table 1.

Table 1 yields mean blueshifts of 0.3874 and 0.6167, which are the blueshifts of PKS 2149–306 and J0332–274, respectively, and mean redshifts of 2.3417 and 1.6227 (without the X-ray line), respectively, which we use as the redshifts of the two objects. Figure 1 shows positions of the identified lines based on the redshifts and blueshifts of the two objects with respect to the observed lines for optical spectra.

The X-ray spectra are shown in Figures 2 and 3 with the positions of lines identified under the blueshift hypothesis with respect to the features observed. In Figure 2 the bottom panel shows the ratios of spectral data from *Chandra* ACIS to the best-fitting power law plus the neutral absorber model. Two other nearby sources with similar X-ray counts, viz., CXOCDFS J033236.8–274407 and CXOCDFS J033213.3–274241, were examined for the purpose of comparison to ensure that the observed feature is not due to the X-ray background or the instrument background. The bottom panel of Figure 3 shows the ratio of Solid-State Imaging Spectrometer (SIS) spectral data to the best-fitting power law plus absorber model. The SIS data of 4U 1957+11, which was observed about 4 days after PKS 2149–306, have also been examined for comparative purposes to ensure that the observed feature is not due to calibration uncertainties.

### 3. DISCUSSION

In PKS 2149–306, the emission feature at 5162 Å identified with C iv  $\lambda$ 1549 has been described (Wilkes 1986) as of “irregular

profile,” which is rather unusual for the very familiar characteristics of the well-known line C iv  $\lambda$ 1549. Also, the strength of the line, viz., the emitted equivalent width of 9.0 Å in the redshift scenario, is rather too small for C iv  $\lambda$ 1549, which is one of the strongest lines in the search list. This raises doubt concerning the

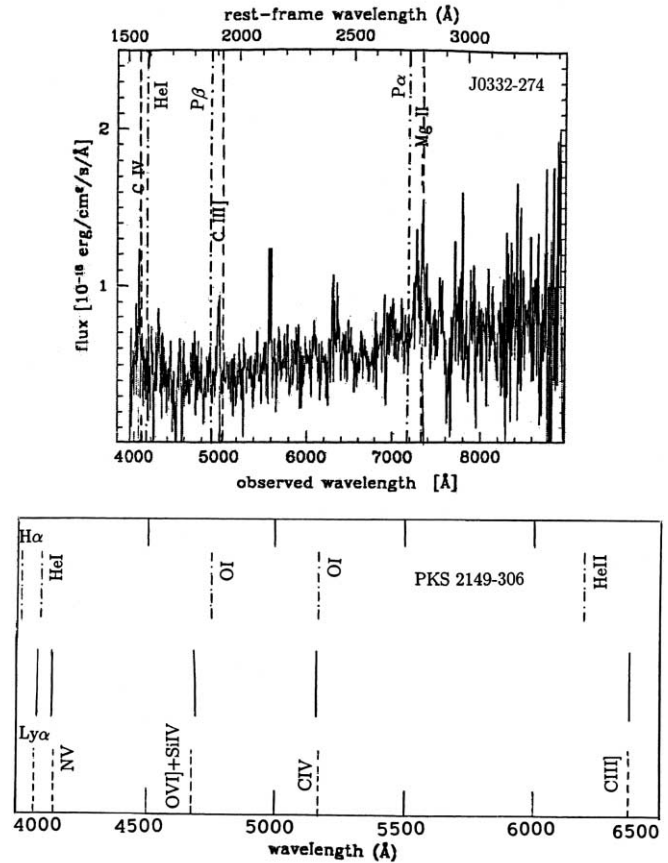


FIG. 1.—Observed optical spectra of J0332–274 (top) and PKS 2149–306 (bottom). The spectrum of J0332–274 is adopted from Wang et al. (2003). The original spectrum of PKS 2149–306 is not available, and the observed wavelengths reported by Wilkes (1986) are shown (solid lines). The positions of identified lines based on the redshift (dashed lines) and blueshift (dot-dashed lines) are also shown for both objects. Redshift and blueshift values assumed here are 1.6227 and 0.6167, respectively, for J0332–274 and 2.3417 and 0.3874, respectively, for PKS 2149–306.

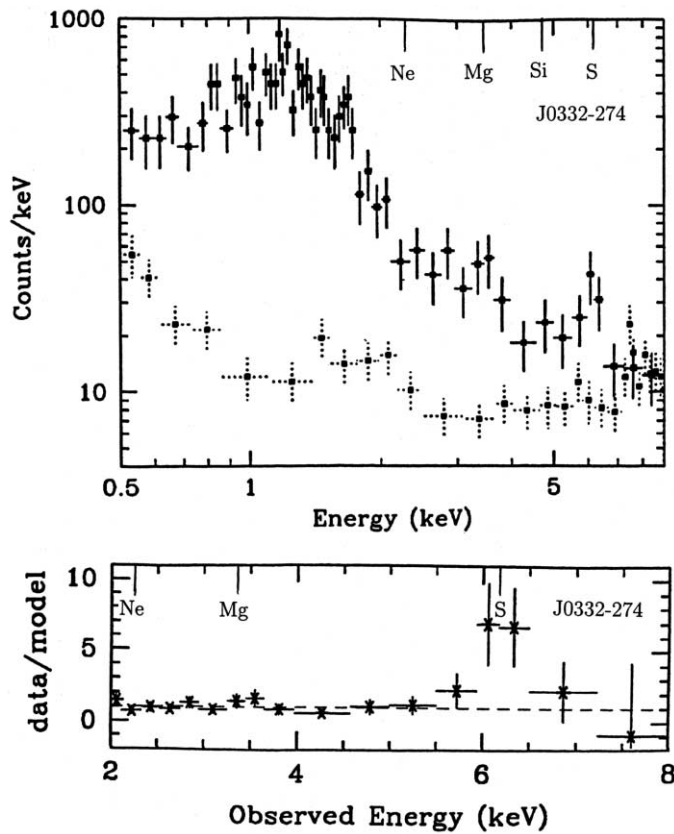


FIG. 2.—Observed X-ray spectrum of J0332–274, adopted from Wang et al. (2003). Filled squares with dotted error bars denote the expected background. Top tick marks denote the positions of  $E_{\text{ob}(03)}$  in Table 2, viz., observed  $K\alpha$  energies for the elements indicated at blueshift 0.6280 (the blueshift of the identified S  $K\alpha$  line).

correctness of the identification. On the other hand, O  $\lambda$ 8449, identified in the blueshift scenario, is known as a broad line of medium strength (see Table 1, Basu & Haque-Copilah 2001).

In J0332–274, the optical feature at 4100 Å has been described as broad (Wang et al. 2003), but its detection is only “marginal,” and it has been identified with C  $\text{IV}$   $\lambda$ 1549 in the redshift hypothesis. However, as mentioned above, the C  $\text{IV}$   $\lambda$ 1549 line is known as one of the strongest emission lines in the search list. It is difficult to conceive that such a strong line will be observed only marginally. The correctness of the identification, once again, is therefore questionable. In the blueshift scenario, this line has been identified with He  $\text{I}$   $\lambda$ 10830, identified in the blueshift scenario, which also, like the O  $\lambda$ 8449 line mentioned above, is known as a broad line of medium strength (see Table 1, Basu & Haque-Copilah 2001). Furthermore, identification of the IR lines P  $\alpha$   $\lambda$ 18751 and P  $\beta$   $\lambda$ 12818, rather than the UV lines Mg  $\text{II}$   $\lambda$ 2798 and C  $\text{III}$   $\lambda$ 1909, respectively, with the observed emission lines has been suggested (Putsil’nik 1979). Moreover, the identification of the X-ray line in the blueshift hypothesis with the  $K\alpha$  line of sulfur, viz., S  $K\alpha$   $\lambda$ 2.3066, gives its emitted equivalent width as only 1.6 keV, which, unlike the corresponding value 11.5 keV in the redshift hypothesis, is not “highly unusual” (see discussion later in this section).

On the other hand, the plasma signature in the spectra of both objects necessitates the exhibition of lines of other elements of lower atomic numbers in the X-ray spectra. Table 2 shows these elements, their atomic numbers  $Z$  and cosmic abundances  $A$ , emitted  $K\alpha$  line energies  $E_e$ , observed  $K\alpha$  line energies  $E_{\text{ob}(21)}$  at blueshift 0.4087 (the same blueshift as that of the identified Ar

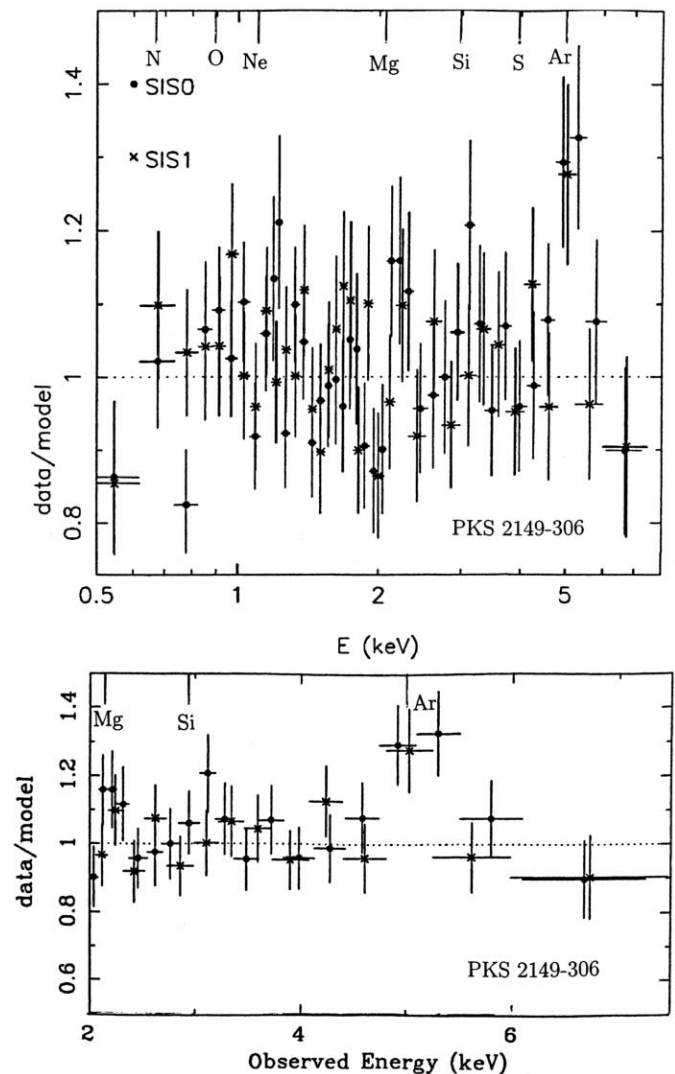


FIG. 3.—Observed X-ray spectrum of PKS 2149–306, adopted from Yaqoob et al. (1999). Top tick marks denote the positions of  $E_{\text{ob}(21)}$  in Table 2, viz., observed  $K\alpha$  energies for the elements indicated at blueshift 0.4087 (the blueshift of the identified Ar  $K\alpha$  line).

TABLE 2  
EXPECTED  $K\alpha$  ENERGIES IN keV

Element	$Z$	$A$	$E_e$	$E_{\text{ob}(21)}$	$E_{\text{ob}(03)}$
C.....	6	8.52	0.2770	0.4685	0.7446 <sup>a</sup>
N.....	7	7.96	0.3924	0.6636 <sup>b</sup>	1.0548 <sup>a</sup>
O.....	8	8.82	0.5249	0.8877 <sup>b</sup>	1.4110 <sup>a</sup>
Ne.....	10	7.92	0.8486	1.4356 <sup>b</sup>	2.2812 <sup>c</sup>
Mg.....	12	7.42	1.2536	2.1201 <sup>b</sup>	3.3700 <sup>c</sup>
Si.....	14	7.52	1.7400	2.9427 <sup>d</sup>	4.6774
S.....	16	7.20	2.3066	3.9009 <sup>d</sup>	6.2000
Ar.....	18	6.80	2.9567	5.000	7.9480
Ca.....	20	6.30	3.6900	6.2405	9.9194
Fe.....	26	7.60	6.4000	10.8236	17.2043

NOTES.— $Z$  is the atomic number;  $A$  is the log abundance by mass on a scale for which H is 12.00 dex (Allen 1973);  $E_e$  is the rest-frame energy (Bearden 1964);  $E_{\text{ob}(21)}$  is the observed energy in PKS 2149–306 at blueshift 0.4087 (the blueshift of the identified Ar  $K\alpha$  line); and  $E_{\text{ob}(03)}$  is the observed energy in J0332–274 at blueshift 0.6280 (the blueshift of the identified S  $K\alpha$  line).

<sup>a</sup> Line seen in Fig. 3 of Wang et al. (2003), in addition to S.

<sup>b</sup> Line seen in Fig. 3 of Yaqoob et al. (1999), in addition to Ar.

<sup>c</sup> Line seen in Fig. 4 of Wang et al. (2003), in addition to S.

<sup>d</sup> Line seen in Fig. 1 of Yaqoob et al. (1999), in addition to Ar.

$K\alpha$  line) for PKS 2149–306, and observed  $K\alpha$  line energies  $E_{\text{ob}(03)}$  at blueshift 0.6280 (the same blueshift as that of the identified S  $K\alpha$  line) for J0332–274. However, it is known that the abundance of each element may vary from object to object, so not all these lines may be seen.

Having said that, some of the lines in Table 2 can indeed be seen around their blueshifted positions, within the wavelength ranges over which the spectra have been published (Figs. 2 and 3). These include low- $Z$  elements N, O, Ne, Mg, Si, and S (C is outside the observed region of the spectrum) in PKS 2149–306 and Ne, Mg, and Si in J0332–274. However, these lines have not been mentioned by the respective authors, perhaps not being considered seriously, as emission features at these energies are not expected in the redshift hypothesis. It may be noted in this connection that similar remarks were also made by Yaqoob et al. (1999) in connection with the X-ray feature in PKS 2149–306, which is probably also present in the *ASCA* observations of Siebert et al. (1996) and Cappi et al. (1997) but was not considered seriously, as an emission feature at that wavelength is not usually expected. Furthermore, it is worth mentioning here in passing that these potential identifications would also hold for the bulk outflow case and could be correct independent of the optical-line identifications, whether the shifts are red or blue.

Fe  $K\alpha$  is located at  $\approx 10.8$  and  $\approx 17.2$  keV in PKS 2149–306 and J0332–274, respectively, as shown in Table 2. Unfortunately, both positions are outside the current observed region, so observations over an extended wavelength (energy) range are recommended for both sources in order to look for the Fe line.

It has been suggested by Matt et al. (1997) that the equivalent widths of the fluorescent lines of Ar and S are so low as not to be detected by currently available detectors, and are expected to be 1–2 orders of magnitude lower than the corresponding features of Fe. But high-quality spectral observations by Ptak et al. (1997) show strong  $K\alpha$  lines of several elements, including S, but no Fe at all in two galaxies: M82 and NGC 253. Unfortunately, the signal-to-noise ratio was not good enough to detect Ar separately, but its abundance relative to solar has been estimated for M82, “tied together” with Ca and Ni, as  $0.22^{+0.14}_{-0.11}$ , and with N, Ca, and Ni for NGC 253 as  $<0.66$ . These are starburst galaxies, and AGNs are probably hidden in the central regions (Ptak et al. 1997). Starburst galaxies are, of course, now known to basically be AGNs (Watabe & Umemura 2005). Figure 3 of Ptak et al. (1997) shows abundance ratios of S/Fe and Ar-Ca-Ni/Fe  $\approx 16$  and 10, respectively, at maximum ranges, for M82. After due consideration of errors involved and suggested possible dust depletion, if any, which may partly “suppress” Fe features, these observations clearly demonstrate that the abundance of Ar and S can really be huge, much higher than that of Fe in some objects, which is very much contrary to the prediction of the model of Matt et al. (1997). Certain assumptions and abundance values used in the model may not be valid for all sources. It can also be noted in this connection that, as shown in Table 2, the cosmic abundance of Fe is only 2.5 and 6.3 times larger than those of S and Ar, respectively. Nevertheless, it would be most interesting to see the strength of the Fe feature when it is detected, if at all, in PKS 2149–306 and J0332–274.

Summing up, we find that the new identifications of the observed lines presented here are free of the inconsistencies of the redshift identifications, which are pointed out earlier in this section, particularly with respect to the C IV line. Finally, the two X-ray lines that could not be identified in the redshift system have been successfully identified in the present analysis based on the blueshift hypothesis.

#### 4. A PROPOSED SCENARIO: THE EJECTION MECHANISM

The so-called slingshot mechanism can eject one or more massive objects from the center of a galaxy when strong interactions near the center make the system gravitationally unstable (Saslaw et al. 1974; Valtonen 1976a, 1976b). It is known that supermassive black holes are seats of activity at the centers of galaxies (Basu et al. 1993). When two galaxies each hosting a supermassive black hole ( $\approx 10^8 M_{\odot}$ ) merge, the initial result (Valtoja et al. 1989) is the formation of a binary system consisting of the two central black holes. It is noteworthy here that a binary black hole system has indeed been discovered in X-rays in NGC 6240 (Komossa et al. 2003). As the merger process proceeds further, a single supermassive black hole may be ejected at a relativistic or nonrelativistic speed, if the two individual black holes are of unequal masses (Mikkola & Valtonen 1990). Again, it is believed (Rees & Saslaw 1975; Lin & Saslaw 1977; De Young 1977) that the black hole located at the center of a galaxy is often surrounded by a gaseous accretion disk, and the disk survives the tidal disruption during the ejection process. Several researchers (Rees 1984; Osterbrock & Mathews 1986; Valtonen & Basu 1991) have shown that the surroundings and the disk associated with the black hole may interact with each other to form an AGN-like object. It is therefore conceivable that PKS 2149–306 and J0332–274 are two such AGNs created by ejection and are moving toward the observer.

#### 5. CONCLUDING REMARKS

The importance of correct identification of observed spectral lines in extragalactic objects is easily appreciated, as it plays the most important role in modern cosmology, which is almost entirely based on redshifts. Redshifts, in turn, are computed from such identifications. Observed lines are routinely identified for determining redshifts; thus, the possibilities of blueshifts have been ignored so far, although it is usually stated that no blueshifts have been detected. It is not the purpose of the present paper to suggest that all or most extragalactic objects are exhibiting blueshifted spectra. However, turning a blind eye to the possibility of blueshifts due to a certain mindset may result in missing a very important cosmological scenario.

The author gratefully acknowledges the valuable and constructive suggestions of two anonymous referees, which led to major improvement in this work.

#### REFERENCES

- Allen, C. W. 1973, *Astrophysical Quantities* (3rd ed.; London: Athlone)
- Basu, D. 1973a, *Nature Phys. Sci.*, 241, 159
- . 1973b, *Observatory*, 93, 229
- . 1998, *Ap&SS*, 259, 415
- . 2000, *Mod. Phys. Lett. A*, 15, 2357
- . 2001a, *Astrophys. Lett. Commun.*, 40, 157
- . 2001b, *Astrophys. Lett. Commun.*, 40, 225
- . 2004, *Phys. Scr.*, 69, 427
- Basu, D., & Haque-Copilah, S. 2001, *Phys. Scr.*, 63, 425
- Basu, D., Valtonen, M. J., Valtonen, H., & Mikkola, S. 1993, *A&A*, 272, 417
- Bearden, J. A. 1964, *X-Ray Wavelengths* (Oak Ridge: AEC)
- Cappi, M., Matsuoka, M., Comastri, A., Brinkmann, W., Elvis, M., Palumbo, G. G. C., & Vignali, C. 1997, *ApJ*, 478, 492
- De Young, D. 1977, *ApJ*, 211, 329
- Giacconi, R., et al. 2002, *ApJS*, 139, 369
- Jauncey, D. L., Batty, M. J., Gulkis, S., & Savage, A. 1982, *AJ*, 87, 763

- Komossa, S., Burwitz, V., Hasinger, G., Predehl, P., Kaastra, J. S., & Ikebe, Y. 2003, *ApJ*, 582, L15
- Lin, D., & Saslaw, W. 1977, *ApJ*, 217, 958
- Matt, G., Fabian, A. C., & Reynolda, C. S. 1997, *MNRAS*, 289, 175
- Mikkola, S., & Valtonen, M. 1990, *ApJ*, 348, 412
- Osterbrock, D., & Mathews, W. 1986, *ARA&A*, 24, 171
- Ptak, A., Serlemitsos, P., Yaqoob, T., Mushotzky, R., & Tsuru, T. 1997, *AJ*, 113, 1286
- Putsil'nik, S. A. 1979, *A&A*, 78, 248
- Rees, M., & Saslaw, W. 1975, *MNRAS*, 171, 53
- Rees, M. J. 1984, *ARA&A*, 22, 471
- Rosati, P., et al. 2002, *ApJ*, 566, 667
- Saslaw, W. C., Valtonen, M. J., & Aarseth, S. J. 1974, *ApJ*, 190, 253
- Siebert, J., Matsuoka, M., Brinkmann, W., Cappi, M., Mihara, T., & Takahashi, T. 1996, *A&A*, 307, 8
- Valtaoja, L., Valtonen, M. J., & Byrd, G. G. 1989, *ApJ*, 343, 47
- Valtonen, M. J. 1976a, *A&A*, 46, 429
- . 1976b, *A&A*, 46, 435
- Valtonen, M. J., & Basu, D. 1991, *J. Astrophys. Astron.*, 12, 91
- Wang, J., et al. 2003, *ApJ*, 590, L87
- Watabe, Y., & Umemura, M. 2005, *ApJ*, 618, 649
- Wilkes, B. 1986, *MNRAS*, 218, 331
- Yaqoob, T., George, I. M., Nandra, K., Turner, T. J., Zobair, S., & Serlemitsos, P. J. 1999, *ApJ*, 525, L9